JACS Au
AN OPEN ACCESS JOURNAL OF THE AMERICAN CHEMICAL SOCIETY

pubs.acs.org/jacsau
Article

An Enzymatic Oxidation Cascade Converts δ-Thiolactone Anthracene to Anthraquinone in the Biosynthesis of Anthraquinone-Fused Enediynes

Published as part of JACS Au virtual special issue "Biocatalysis in Asia and Pacific".

Guang-Lei Ma,[#] Wan-Qiu Liu,[#] Huawei Huang, Xin-Fu Yan, Wei Shen, Surawit Visitsatthawong, Kridsadakorn Prakinee, Hoa Tran, Xiaohui Fan, Yong-Gui Gao, Pimchai Chaiyen, Jian Li,* and Zhao-Xun Liang*

Cite This: *JACS Au* 2024, 4, 2925−2935

Read Online

ACCESS | Metrics & More | Article Recommendations | Supporting Information

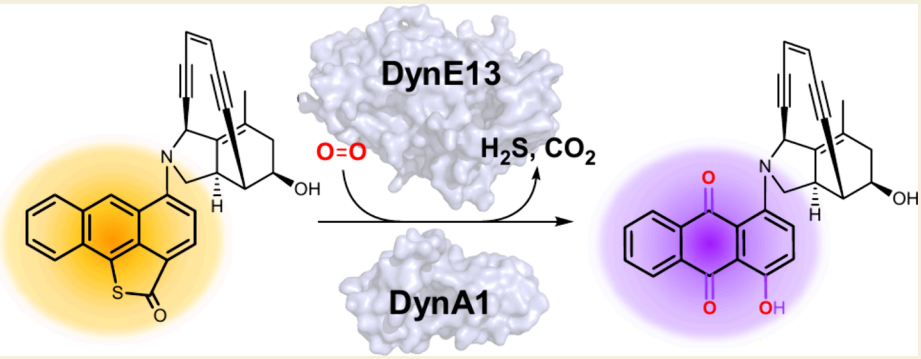

ABSTRACT: Anthraquinone-fused enediynes are anticancer natural products featuring a DNA-intercalating anthraquinone moiety. Despite recent insights into anthraquinone-fused enediyne (AQE) biosynthesis, the enzymatic steps involved in anthraquinone biogenesis remain to be elucidated. Through a combination of *in vitro* and *in vivo* studies, we demonstrated that a two-enzyme system, composed of a flavin adenine dinucleotide (FAD)-dependent monooxygenase (DynE13) and a cofactor-free enzyme (DynA1), catalyzes the final steps of anthraquinone formation by converting δ-thiolactone anthracene to hydroxyanthraquinone. We showed that the three oxygen atoms in the hydroxyanthraquinone originate from molecular oxygen (O_2), with the sulfur atom eliminated as H_2S. We further identified the key catalytic residues of DynE13 and A1 by structural and site-directed mutagenesis studies. Our data support a catalytic mechanism wherein DynE13 installs two oxygen atoms with concurrent desulfurization and decarboxylation, whereas DynA1 acts as a cofactor-free monooxygenase, installing the final oxygen atom in the hydroxyanthraquinone. These findings establish the indispensable roles of DynE13 and DynA1 in AQE biosynthesis and unveil novel enzymatic strategies for anthraquinone formation.

KEYWORDS: *enediynes, anthraquinone formation, δ-thiolactone*

INTRODUCTION

Enediynes are a family of highly cytotoxic bacterial natural products characterized by a unique 1,5-diyne-3-ene bicyclic structure embedded in a 9- or 10-membered enediyne core.[1−7] Among the known enediynes, the anthraquinone-fused enediynes (AQEs or AFEs) are renowned for their distinctive molecular architecture consisting of an anthraquinone moiety fused to the 10-membered enediyne warhead, as exemplified by dynemicin A (Figure 1 and Scheme S1).[1,2,8−12] The anthraquinone moiety serves a dual role: it contributes to the DNA-binding ability of AQEs through intercalation and also serves as a trigger device as the reduction of anthraquinone initiates the Bergmann cyclization to produce a diradical species, resulting in DNA damage and subsequent cell death.[13−16]

The biosynthesis of AQEs has attracted great attention since the first discovery of dynemicins, and studies over the last several years have yielded a flurry of fresh insights into the

Received: March 28, 2024
Revised: May 31, 2024
Accepted: July 5, 2024
Published: August 9, 2024

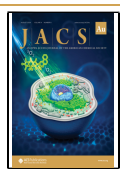

https://doi.org/10.1021/jacsau.4c00279
JACS Au 2024, 4, 2925−2935

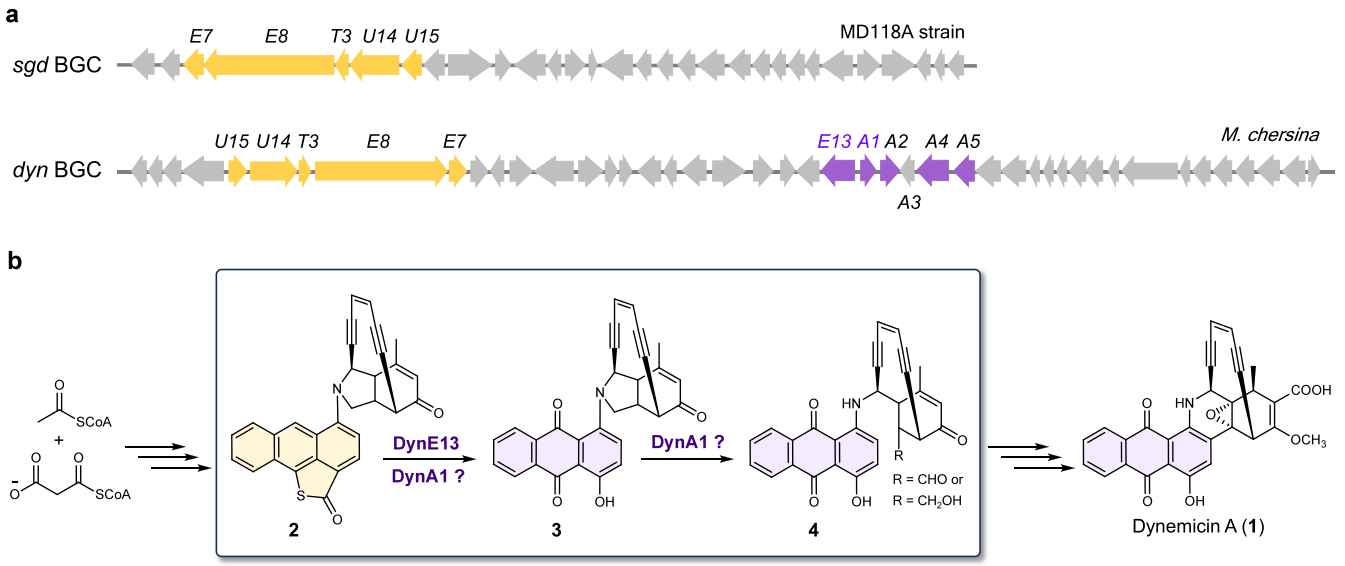

Figure 1. AQE biosynthetic gene clusters (BGCs) and the putative roles of DynE13 and DynA1 in AQE biosynthesis. (a) BGCs for sungeidine (*sgd*) and dynemicin (*dyn*) biosynthesis. *sgd* BGC lacks several genes (shown in violet) that are conserved in *dyn* and other canonical AQE BGCs. The warhead cassette genes essential for enediyne biosynthesis are shown in yellow. (b) The putative function of DynE13 and A1 is based on previous *in vivo* gene knockout and pathway retrofitting studies.[20,22,23]

biosynthetic mechanism of AQEs.[17−25] Early genome sequencing revealed that the AQE biosynthetic gene clusters (BGCs) contain an essential warhead gene cassette (e.g., *dynE8*, *E7*, *T3*, *U14*, *U15*) and other ancillary genes (Figure 1a).[11,12,26] The conserved iterative type-I enediyne polyketide synthase (PKSE, e.g., DynE8) is likely to initiate the biosynthesis of the enediyne warhead.[24,27,28] Experimental evidence suggests that the anthraquinone moiety of AQEs also originates from the PKSE product and a δ-thiolactone iodoanthracene intermediate.[21,25] Surprisingly, the biosynthesis of the polyketide-derived AQEs do not utilize a nonreducing iterative polyketide synthase (PKS), commonly found in many anthraquinone biosynthetic pathways.[29] We recently reported a degenerative AQE biosynthetic pathway that produces a group of compounds named sungeidines. Unlike dynemicins, sungeidines feature a δ-thiolactone anthracene moiety instead of an anthraquinone (Scheme S2).[30] We demonstrated that the sungeidine pathway can be "resurrected" to produce the anthraquinone-containing AQE scaffold when retrofitted with six dyn genes (*dynE13*, *A1*−*A5*; Figure 1a).[22] Based on the cycloaromatized products produced by the retrofitted pathways, the biosynthetic steps and intermediates were proposed for the late stage of AQE biosynthesis (Scheme S3).[22]

From our retrofitting experiment and the gene knockout experiments from Ma et al. and Cohen and Townsend,[22,23] it was concluded that AQE biosynthesis involves the conversion of a δ-thiolactone anthracene to anthraquinone (e.g., **3**). The experiments also implicated DynE13, a putative flavin-dependent enzyme, and DynA1, an AclR/SnoaL-like protein, in the conversion of δ-thiolactone anthracene to anthraquinone.[26,31,32] The *in vivo* experiments also suggested that DynA1 may be involved in the cleavage of a C−N bond to generate another biosynthetic intermediate that resembles **4** (Figure 1b).[20,22] Given the complex background of the cellular environment, the functions of DynE13 and DynA1 remain speculative, with their catalytic roles remaining to be fully established. Our early effort to validate the enzymatic function of DynE13 by *in vitro* assays was hindered by the difficulty of expressing the recombinant protein.

In this study, we redesigned the protein construct and optimized the expression conditions to produce solubilizing protein-tagged recombinant DynE13. The access to recombinant DynE13 and A1 allowed us to perform enzymatic assays to demonstrate their enzymatic activity under *in vitro* conditions. We concluded that DynE13 and DynA1 are the only enzymes required to transform the δ-thiolactone anthracene to anthraquinone, with the two enzymes catalyzing a cascade of oxidation, desulfurization, and decarboxylation reactions. Our structural and mechanistic studies also yield insights into the multistep catalytic mechanism and the origin of the oxygen atoms, as well as the fate of the sulfur atom in the δ-thiolactone anthracene.

RESULTS

In Vitro Reconstitution of the Enzymatic Activity of DynE13 and DynA1 Using a Cell-Free System

The expression and production of recombinant N-terminal $(His)_6$-tagged DynA1 proceeded smoothly, leading to the purification of a homodimeric DynA1 to homogeneity via size-exclusion chromatography (Figure S1). However, initial attempts to produce recombinant DynE13 in *Escherichia coli* using either the original or codon-optimized DNA sequence were unsuccessful, as no noticeable expression of DynE13 was observed. Screening various solubilizing tags and protein constructs with truncated C- or N-terminal regions revealed that the N-terminal SUMO-tagged DynE13 was expressed, as confirmed by Western blotting and SDS-PAGE gel electrophoresis (data not shown). The SUMO-tagged DynE13 was only partially soluble under all of the conditions we tested, with approximately one-third of the protein present in the soluble fraction. The soluble fraction exhibited a high propensity for aggregation, hindering further purification of the protein for *in vitro* enzymatic assays.

Cell-free systems utilizing *E. coli* and other expression hosts have emerged as useful tools.[33−35] Because recombinant

https://doi.org/10.1021/jacsau.4c00279
JACS Au 2024, 4, 2925−2935

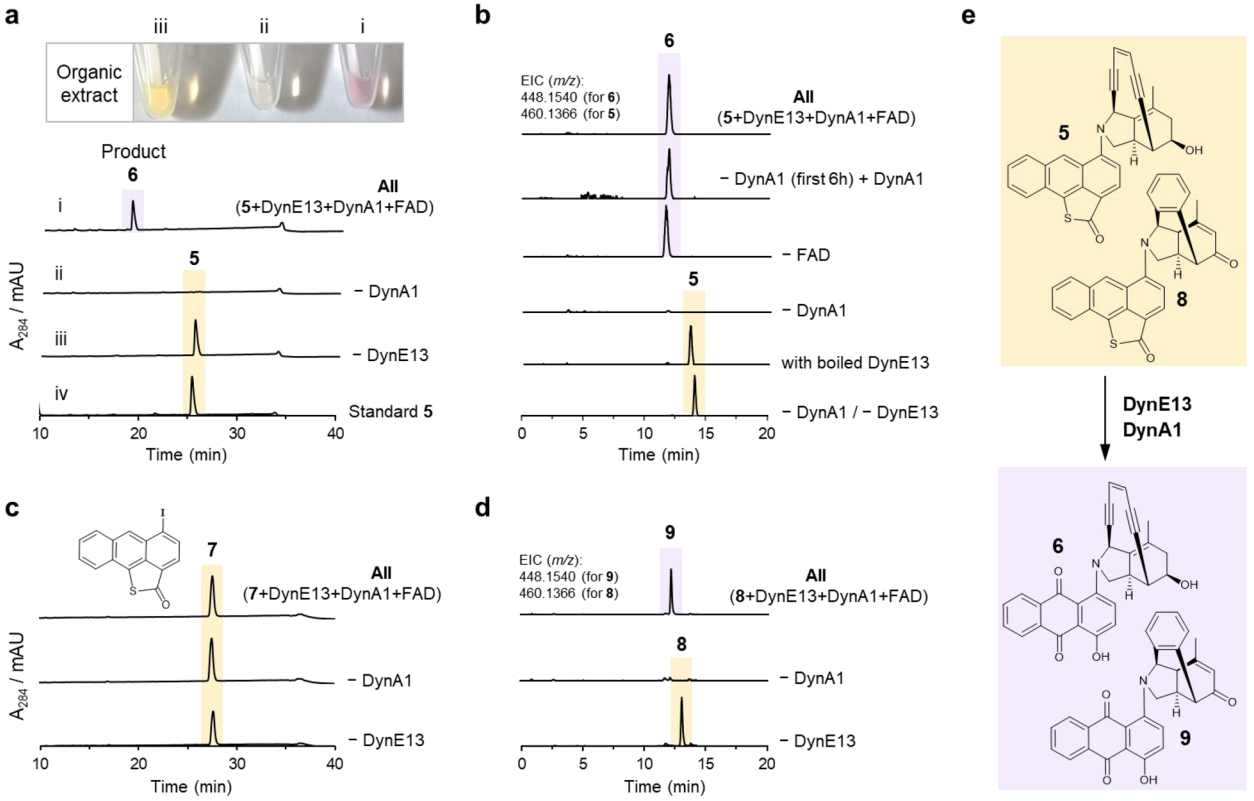

Figure 2. *In vitro* enzymatic assays for DynE13 and DynA1. (a,b) The HPLC analysis of the enzymatic conversion of **5** to **6** was performed using the cell-free system (a) and purified enzymes (b). (c) HPLC analysis of the enzymatic activity of DynE13 and DynA1 using **7** as the substrate using the cell-free system. (d) HPLC analysis of the enzymatic conversion of **8** to **9** using the cell-free system. Note that the samples in panels (a) or (c) and (b) or (d) were analyzed by using different HPLC elution conditions. The UV–vis detector of the HPLC was set at 284 nm. (e) Structures of the enzymatic substrates and products.

proteins are produced extracellularly, cell-free systems offer advantages in generating functional proteins that may not be achievable by intracellular expression. Our preliminary investigations indicated that SUMO-tagged DynE13 could be expressed extracellularly in an *E. coli*-based cell-free system. Upon the addition of compound **5**, which was obtained previously by fermentation,[22,23] to the cell-free mixture containing DynE13 and DynA1-expressing plasmids, FAD^+, NADH, and the flavin reductase StyB,[36] a visible color change from orange to violet occurred over time (Figure 2a). Because the anthraquinone chromophore exhibits an intense violet color,[22] the change in coloration suggests the likely conversion of the *δ*-thiolactone anthracene substrate to anthraquinone in the cell-free system. An HPLC analysis of the reaction mixture revealed a new compound with a mass of 448.1540 *m*/*z* ($C_{29}H_{22}NO_4$, $[M + H]^+$) and a UV–vis spectrum ($\lambda_{max} \sim 536$ nm) characteristic of anticipated anthraquinone product **6** (Figure 2e). The product's identity was further supported by a detailed MS/MS analysis and comparison with previously published data (Scheme S4).[23] Intriguingly, when only DynE13, but not DynA1, was expressed, substrate **5** was consumed, yet no products were detected (Figure 2a). This puzzling observation aligns with our previous *in vivo* pathway retrofitting experiment, which showed that the overexpression of DynE13 in the sungeidine-producing *Micromonospora* sp. MD118A alone resulted in the abolishment of sungeidine production, but without yielding any new isolatable metabolites.[22]

We further tested whether DynE13 could process *δ*-thiolactone iodoanthracene **7** (i.e., 5-iodo-2*H*-anthra[9,1-*bc*]thiophen-2-one) and **8** (the cycloaromatized derivative of **2**) as substrates. Our results indicate that while DynE13 could turn over compound **8**, it did not exhibit activity toward **7** (Figure 2c,d).

This enzymatic reaction with **8** generated a product with a mass of 448.1531 *m*/*z* ($[M + H]^+$) and UV–vis absorbance consistent with anthraquinone derivative **9** (Figure 2d,e and Scheme S5). These findings suggest that the amino-containing bicyclic enediyne or its cycloaromatized form is essential for DynE13 recognition.

In Vitro Reconstitution of the Enzymatic Activity of DynE13 and DynA1 Using Purified Enzymes

The cell lysate used in the cell-free system-based assays presents a highly complex mixture of chemical and biological components that potentially interfere with the enzymatic reactions catalyzed by DynE13 and A1. To unambiguously establish the enzymatic function of DynE13 and DynA1 and to delve into the mechanism of the enzymatic reaction, an enzymatic assay using purified enzymes remains the preferred approach. We explored various strategies to improve the expression yield and enhance the solubility of recombinant DynE13. Coexpression with the protein-folding chaperone (pG-KJE8[37]) and refinement of purification conditions yielded successful expression and purification of the SUMO-tagged DynE13 as a monomeric protein in the solution (refer to Figure S2). The enzyme solution displayed a yellow hue, indicating copurification of the flavin cofactor. An LC–MS

https://doi.org/10.1021/jacsau.4c00279
JACS Au 2024, 4, 2925–2935

analysis of the denatured enzyme confirmed the presence of flavin adenine dinucleotide (FAD) and flavin mononucleotide (FMN) bound to the enzyme, with the two cofactors coexisting in approximately a 1:1 ratio (refer to Figure S3). This observation aligns with the fact that DynE13 demonstrates nearly similar enzymatic activity with or without exogenous flavin (FAD or FMN). Given the sequence homology shared by DynE13 and other FAD-dependent monooxygenases, FAD is presumed to be the biologically relevant cofactor.

For *in vitro* enzymatic assays, we simplified the reaction mixture by substituting the StyB-based cofactor regeneration system with a small molecule (1-benzyl-1,4-dihydroicotinamide, BNAH), as described in previous studies.[38] Additionally, catalase was incorporated to counteract any potential adverse effects caused by hydrogen peroxide produced during the flavin-mediated enzymatic reaction. The enzymatic assays showed that newly prepared DynE13 and DynA1 effectively converted substrate **5** into product **6** (Figure 2b). DynE13 alone seemed to deplete the substrate without yielding any detectable products, consistent with the earlier observations from the enzymatic assays conducted using the cell-free system.

When DynE13 and substrate **5** were incubated for 6 h followed by the addition of DynA1 into the reaction solution, we observed the formation of product **6** (Figure 2b). This observation suggests that DynE13's product is present in the reaction solution, but it could not be isolated or detected by the HPLC or LC−MS method. These findings, combined with those from the cell-free system, support the notion that DynE13 and DynA1 are solely responsible for the transformation of the *δ*-thiolactone anthracene moiety into hydroxyanthraquinone in AQE biosynthesis, with DynE13 likely acting on the substrate before DynA1 (Figure 2e).

Feeding Experiments Support the Role of DynE13 and DynA1 in Anthraquinone Formation

We conducted further experiments to test whether DynE13 and A1 could catalyze the turnover of substrate **5** under *in vivo* conditions. We supplied **5** to *Micromonospora* sp. MD118 mutants that overexpress *dynE13*, *dynE13/A1*, or *dynA1/A2*. The feeding experiments showed that **5** was consumed by the MD118AΔΔ::*dynE13* and MD118AΔΔ::*dynE13/A1* strains, but not the MD118AΔΔ::*dynA1/A2* strain. We also found that MD118AΔΔ::*dynE13/A1*, but not the MD118AΔΔ::*dynE13* strain, produced a new fermentation product (**10**) when the culture medium was supplemented with compound **5** (Figure 3). The identity of product **10** was established as 1-amino-4-hydroxyanthraquinone by comparison with an authentic standard (Scheme S6).[39] Earlier reports by Cohen and Townsend suggested that **5** was turned over by the dynemicin-producing strain *Micromonospora chersina* to the anthraquinone-containing **6**.[23] Product **10** was most likely generated by the *in vivo* decomposition of the anthraquinone-containing **6**, further supporting the conclusion that the DynE13/DynA1 pair is responsible for the conversion of *δ*-thiolactone anthracene to anthraquinone in AQE biosynthesis.

The Oxygen Atoms of Hydroxyanthraquinone Originate from Molecular Oxygen

After establishing the enzymatic function of DynE13/A1, we proceeded to investigate their catalytic mechanism by first probing the origin of oxygen atoms in anthraquinone. *In vitro* enzymatic assays were conducted by performing the DynE13/A1 enzymatic reaction either under an $^{18}O_2$ atmosphere or in a $H_2{}^{18}O$ solution. Under the $^{18}O_2$ atmosphere, the M + 6 peak (m/z 454.1678) and M + 4 peak (m/z 452.1640) replaced the M peak (m/z 448.1548) as the prominent peaks, suggesting the incorporation of three or two ^{18}O atoms. For the $H_2{}^{18}O$-labeling reaction, the presence of ∼50% $H_2{}^{18}O$ in the cell-free system-based assay resulted in only a slight increase in the M + 2 peak to indicate the incorporation of an ^{18}O atom. In comparison, the assays using purified enzymes with a high concentration of $H_2{}^{18}O$ (>90%) resulted in a significant increase in the M + 2 isotopic peak (Figure 4a). The observed discrepancy in ^{18}O-incorporating efficiency between the cell-free system and purified enzyme-based experiments likely reflects the differences in the $H_2{}^{18}O$ concentration, the FAD/FMN cofactor ratio, and the enzymatic reaction conditions. The observed isotopic shifts in the $^{18}O_2$- and $H_2{}^{18}O$-labeling experiments indicate that the three oxygen atoms in the hydroxyanthraquinone originate from molecular oxygen, with one oxygen atom likely incorporated in the product not directly from O_2, but from an $H_2{}^{18}O$ byproduct as we will detail in the Discussion section (Figure 4a,d). The ^{18}O-labeling results corroborate the earlier findings by Cohen and Townsend, who drew similar conclusions based on the fermentation of *M. chersina* under the $^{18}O_2$ atmosphere.[24] The incorporation of ^{18}O into the hydroxyanthraquinone moiety also confirms that the biosynthesis of AQE differs from type-II PKS-mediated anthraquinone biosynthesis whereby one of the two quinone oxygen atoms typically derives from acetate.[40−42]

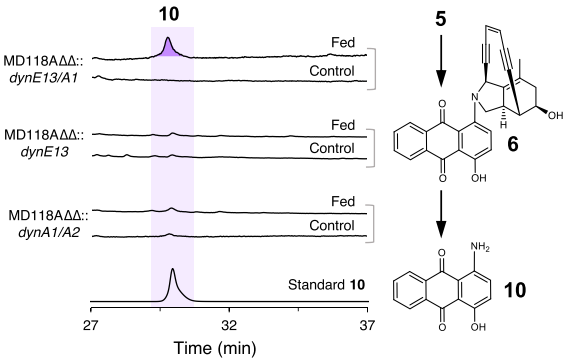

Figure 3. HPLC analysis of *in vivo* conversion of **5** in *Micromonospora* sp. MD118A mutant strains. The mutant strains were fermented in an M5 culture medium without adding the iodide salt that is essential for Sgd and Dyn production. The HPLC detector was set to 550 nm.

The Sulfur Atom Was Eliminated as H_2S during the DynE13-Catalyzed Reaction

The conversion of *δ*-thiolactone anthracene **5** to hydroxyanthraquinone **6** requires removal of the *δ*-thiolactone moiety via the cleavage of two C−S bonds. To the best of our knowledge, a flavin enzyme catalyzing such a desulfurization reaction is unprecedented. We hypothesized that *δ*-thiolactone could undergo hydrolysis, releasing the sulfur atom as hydrogen sulfide (H_2S), with the carboxylate subsequently removed via decarboxylation. While rare, the production of H_2S as a byproduct has been documented in other biosynthetic pathways.[43,44] Alternatively, the *δ*-thiolactone could be removed without breaking one of the C−S bonds, yielding carbonyl sulfide (COS or O═C═S) as a byproduct.

To test whether the enzymatic reactions produce H_2S, we employed monobromobimane (MBB) as a trapping agent to

https://doi.org/10.1021/jacsau.4c00279
JACS Au 2024, 4, 2925−2935

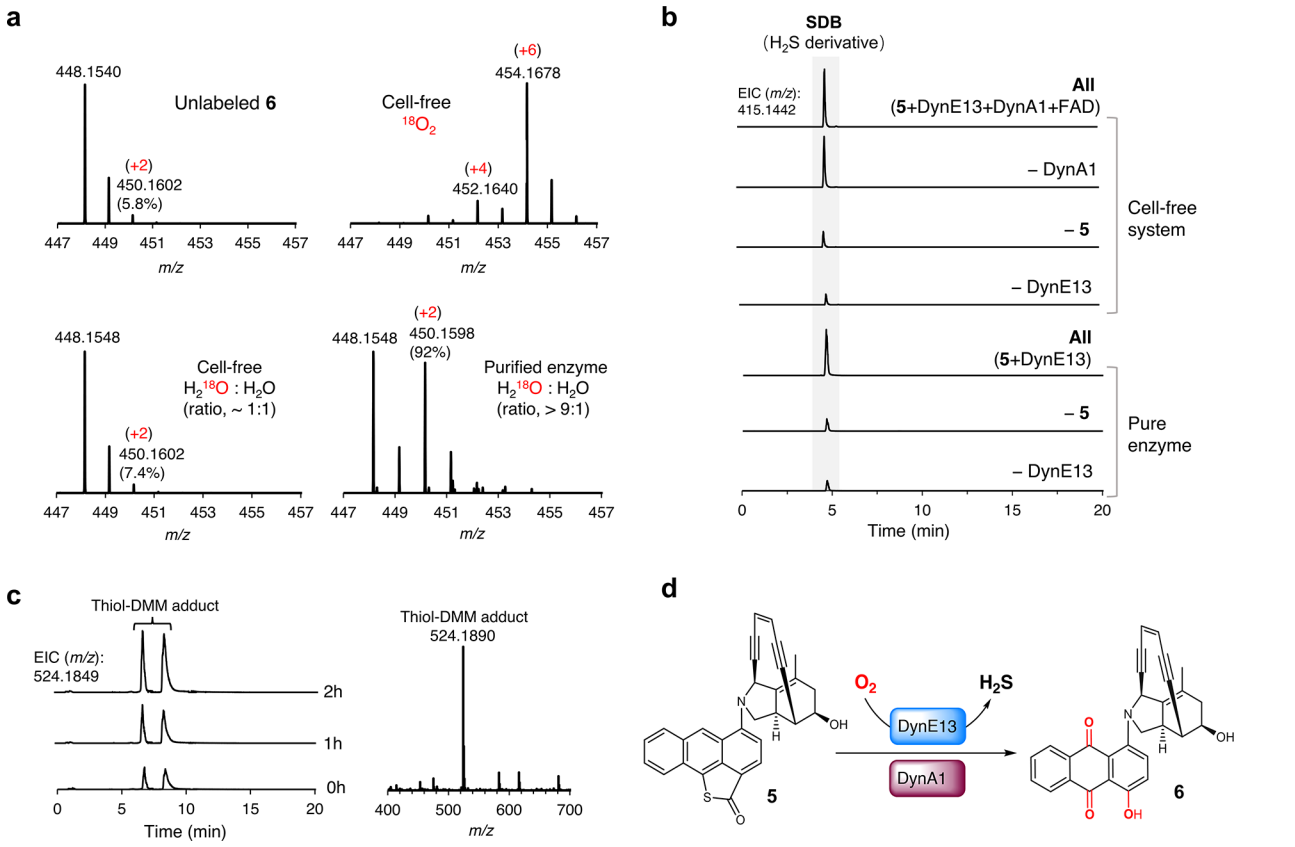

Figure 4. Experiments to determine the origin of the oxygen atoms in the hydroxyanthraquinone moiety and the fate of the sulfur in *δ*-thiolactone anthracene. (a) LC−MS analysis of product **6** in $^{18}O_2$- and $H_2{}^{18}O$-labeling experiments. The $^{18}O_2$-labeling experiment was performed in a cell-free system, while the $H_2{}^{18}O$ experiment was first conducted in the cell-free system (approximate $H_2{}^{18}O/H_2O$ ratio 1:1) and then using purified enzymes ($H_2{}^{18}O/H_2O$ ratio >9:1). (b) Detection of the byproduct H_2S in the DynE13-catalyzed reaction (at a 1 h time point) using the monobromobimane (MBB)-based derivatization method.[45] (c) Detection of H_2S production in the DynE13-catalyzed reaction with the mass spectrum of thiol-DMM adduct shown. The detection of H_2S was performed using an enzyme-coupled method (Scheme S8).[46] (d) Origin of oxygen atoms and the fate of the sulfur group in the anthraquinone biosynthesis from **5** to **6**.

capture H_2S, forming the stable sulfide dibimane (SDB; see Scheme S7).[45] Since the reaction of MBB with H_2S must be performed under anaerobic conditions, we first conducted the enzymatic reactions aerobically to allow FAD-facilitated substrate oxidation and then introduced MBB into the reaction mixture within an anaerobic chamber. Comparative analysis against the controls revealed significantly higher levels of H_2S detected in both the cell-free system and the pure enzyme system-based assays (Figure 4b).

To further confirm the production of H_2S as a byproduct, we used an alternative enzyme-coupled method that relies on the *O*-acetylserine sulfhydrylase (i.e., CysM) that catalyzes the reaction between hydrogen sulfide (HS^-) and *O*-acetyl serine to form L-cysteine.[46] The L-cysteine is then derivatized with the thiol-reactive DMM (i.e., 7-diethylamino-3-(4-maleimidophenyl)-4-methylcoumarin) to generate a thiol-DMM adduct (shown as two peaks due to an equilibrium between the protonated and deprotonated forms) that can be detected easily by HPLC (Scheme S9). Using this enzyme-coupled method, we observed time-dependent H_2S production (Figure 4c). Importantly, H_2S was produced even in the presence of DynE13 and in the absence of DynA1 (Figure 4b), suggesting that C−S bond cleavage and desulfurization occurred during the DynE13-catalyzed reaction.

Mapping the Catalytic Residues of DynE13 and DynA1

Considering the unusual chemical transformation catalyzed by DynE13, obtaining the crystal structure of DynE13 would provide insights into its potentially novel catalytic mechanism. However, crystallizing DynE13 proved to be challenging due to its propensity to aggregate at high protein concentrations. Instead, we employed AlphaFold2[47] to construct a structural model of DynE13 and manually incorporated the cofactor FAD. The resulting model revealed a well-defined pocket adjacent to the isoalloxazine ring of FAD (Figure 5a). Substrate **5** could snugly fit into this pocket, with the *δ*-thiolactone anthracene moiety positioned in proximity to several polar residues (C297, Y216, Y179, and T46) that are conserved in DynE13 and its homologues (see Figure S4). To investigate the potential involvement of these residues in catalysis, we generated the four single mutants (C297A, Y216F, Y179F, and T46A) and conducted *in vitro* enzymatic assays. The assay results suggest that none of the four residues seem to be essential for the enzymatic function, as all four single mutants exhibited enzymatic activity. However, the turnover rate of the substrate by the T46A and Y179F mutants was significantly lower than that of DynE13 (Figure 5b), suggesting that the two residues are likely to play some kind of catalytic roles in DynE13.

For DynA1, we successfully crystallized the protein for X-ray diffraction experiments, obtaining the *apo*-protein structure at

https://doi.org/10.1021/jacsau.4c00279
JACS Au 2024, 4, 2925−2935

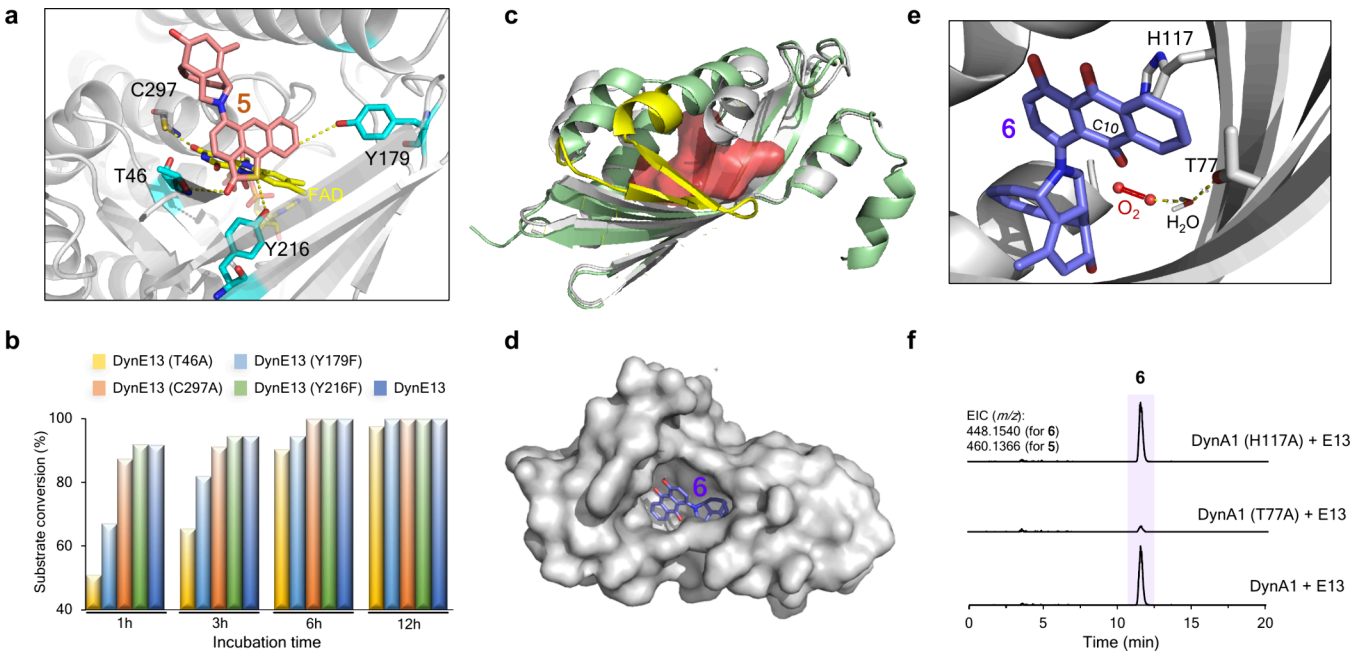

Figure 5. Identification of the catalytic residues of DynE13 and DynA1. (a) Model of the DynE13−substrate complex showing the four potential catalytic residues positioned in the proximity of substrate **5**. (b) Relative enzymatic activity of DynE13 mutants (T46A, Y179F, C297A, and Y216F). Substrate conversion was monitored by HPLC (Scheme S9). (c) Crystal structure of *apo*-DynA1 (gray) superimposed on the DynA1 model (pale green) generated by AlphaFold2. The 19-residue motif missing in the crystal structure is shown in yellow. The putative substrate-binding pocket is shown as an orange blob. (d,e) Computational docking generated a model of the DynA1−product complex with the two potential catalytic residues highlighted. The O_2 and H_2O molecules were modeled manually with the molecules connected by a hydrogen-bonding network. (f) HPLC analysis of the enzymatic activity of DynA1 and the two single mutants.

a resolution of 2.38 Å (Figure 5c). The electron density for a 19-residue motif (aa30−aa48) was absent in the density map, likely due to the flexibility of this motif that may act as a lid for the substrate-binding pocket. The *apo*-structure adopts a *β*-barrel fold that contains a spacious ligand-binding pocket, reminiscent of those found in its homologous enzymes such as SnoL, AclR, and IdmH (Figure 5c,d).[31,48] Attempts to cocrystallize DynA1 with compounds **5**, **7**, and **8** did not result in the formation of *holo*-DynA1 with the ligands bound. We employed computational docking to generate a model for the enzyme−product (**6**) complex. Two conserved polar residues (H117 and T77) positioned adjacent to the anthraquinone moiety were identified as potential catalytic residues (Figure 5e). We prepared the two single mutants, H117A and T77A, for enzyme activity assays. While the H117A mutation did not seem to affect the enzymatic activity of DynA1, the T77A mutation nearly abolished the catalytic activity (Figure 5f). With a water molecule-mediated hydrogen-bond network between O_2 and T77, an O_2 molecule can be modeled into the structure with the O_2 positioned next to the oxygenation site (C10) of **6** (Figure 5e). These observations unveil the essential role of T77 as a catalytic residue and underscore the importance of the catalytically active site of DynA1 for the biogenesis of the anthraquinone moiety.

Considering the sequence and structural homology shared by DynA1 and the cofactor-free oxygenases,[49,50] we tested whether DynA1 could oxygenate structurally simple non-native substrates. We found that DynA1 could convert anthrone to the dimeric product bianthronyl via C−C bond formation under aerobic conditions (Scheme S9). The formation of bianthronyl is likely to involve the oxidative formation of a carbon-centered radical at the C10 position, which may also occur during the catalytic turnover of the native substrate of DynA1 as we discuss below.

DISCUSSION

The experimental findings presented above support the roles of DynE13 and DynA1 in orchestrating the final steps of hydroxyanthraquinone formation in AQE biosynthesis. Our investigations affirm that the two enzymes collectively transform *δ*-thiolactone anthracene into hydroxyanthraquinone, firmly establishing DynE13 as a flavin-dependent oxygenase in anthraquinone biogenesis. Our early *in vivo* studies implied the involvement of DynA1 in the conversion of compounds **2** to **3** and potentially in the conversion of **3** to **4** (Figure 1b).[22] However, we did not observe the production of **4** by DynE13/A1 under *in vitro* conditions, suggesting that DynA1 primarily contributes to the biogenesis of the hydroxyanthraquinone moiety. Recent work by Shen and colleagues demonstrated that gene deletion in the tiancimycin-A pathway in *Streptomyces* sp. CB03234 resulted in the production of TNM H, an on-path biosynthetic intermediate structurally resembling compound **4** but with an aldehyde group instead of a hydroxyl group at the C8 position.[20] The production of **4** by the *Micromonospora* sp. MD118A *dynE13/A1*-overexpressing strain may involve other enzymes, including a nonspecific aldehyde reductase, a phenomenon well-documented in bacteria.[51] Despite our extensive efforts, we encountered challenges in isolating and characterizing the enzymatic product of DynE13, from both the fermentation culture and the *in vitro* enzymatic assay solution. A perplexing observation first emerged when we noted that overexpression of DynE13 in the *Micromonospora* sp. MD118 led to the depletion of the upstream biosynthetic intermediate and its

https://doi.org/10.1021/jacsau.4c00279
JACS Au 2024, 4, 2925−2935

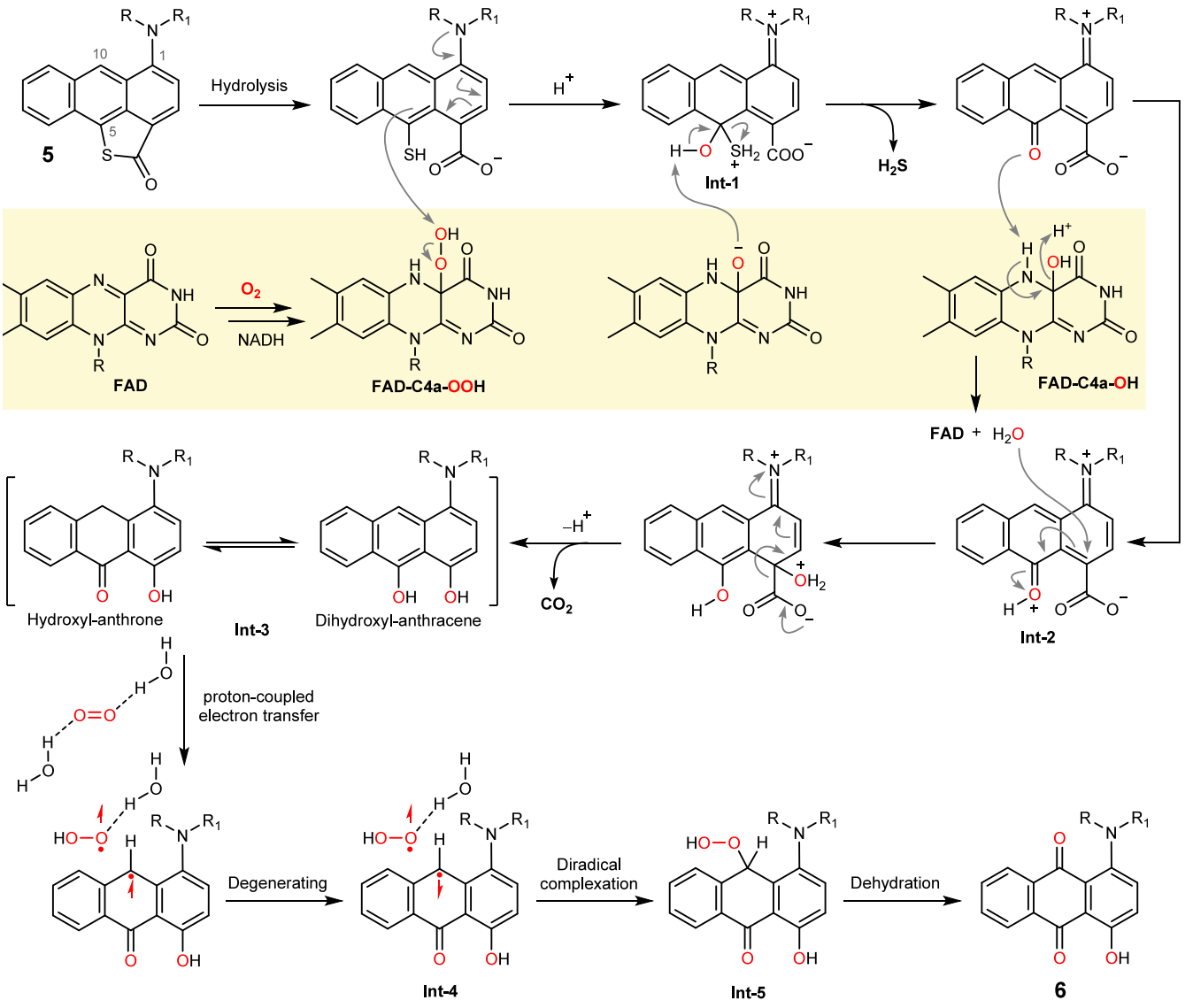

Figure 6. Hypothetical mechanism for the DynE13- and DynA1-catalyzed transformation of *δ*-thiolactone anthracene into hydroxyanthraquinone. The oxygenation of *δ*-thiolactone anthracene at C5 and C3 is catalyzed by the flavo-oxygenase DynE13. The oxygenation at C10 is catalyzed by the cofactor-free oxygenase DynA1.

sungeidine derivatives without yielding any discernible downstream products.[22] This led us to speculate previously that DynE13 might form a covalent adduct with the substrate, necessitating the presence of downstream enzyme DynA1 to facilitate the release of the free product. However, insights gleaned from our current *in vitro* enzymatic assays suggest a different scenario. It seems more plausible that DynE13 generates a freestanding product that is highly susceptible to degradation or polymerization during the organic extraction or chromatographic isolation processes, which are inevitably needed for the characterization of the enzymatic products.

In addition to establishing the roles of DynE13 and DynA1 in AQE biosynthesis, this study provides mechanistic insight into the enzymatic transformation of *δ*-thiolactone anthracene to hydroxyanthraquinone. The remarkable structural transformation requires a series of oxidation steps alongside C−S and C−C bond cleavage. Based on the information gathered from our *in vitro* and *in vivo* experiments, we proposed a hypothetical mechanism to rationalize how the two enzymes catalyze such a multistep transformation. In the hypothetical mechanism (Figure 6a), DynE13 initiates the process by first promoting the hydrolysis of the thiolactone, followed by hydroperoxyl-flavin-mediated hydroxylation at the carbon adjacent to the sulfur atom. The resulting germinal diol-like intermediate (Int-1) collapses, leading to the cleavage of the C−S bond and release of H_2S. T46 is presumed to participate in these catalytic steps due to its proximity to the thiolactone according to the structural model (Figure 5a). In the next step, deprotonation of N5 of the isoalloxazine ring leads to the release of H_2O from C4a to regenerate the oxidized flavin. The newly released H_2O reacts with the intermediate (Int-2) through a 1,4-nucleophilic addition reaction to install the second hydroxyl group. This proposal is supported by our ^{18}O-isotope experiments that show that the solvent H_2O can compete with the oxygen-derived H_2O during the installation of the second hydroxyl group (Figure 4a). This nucleophilic addition reaction entails a facile decarboxylation reaction facilitated by the positively charged amine as the electron sink (Figure 6). The speculated final product (Int-3) of DynE13 contains a 1,9-anthracenediol moiety that has never been

https://doi.org/10.1021/jacsau.4c00279
JACS Au 2024, 4, 2925−2935

chemically synthesized or characterized to our knowledge. This is probably because anthracenediols are generally susceptible to photo-oxidation and polymerization,[52−54] which may explain why the product of DynE13 could not be isolated or detected by conventional HPLC or LC−MS methods.

Overall, DynE13 orchestrates two hydroxylation events at two carbon sites along with concurrent decarboxylation and desulfurization reactions. The proposed mechanism suggests that DynE13 functions as a flavoprotein dioxygenase, wherein both oxygen atoms from oxygen gas are incorporated into the substrate via C4a−OOH hydroxylation and subsequent C4a−OH dehydration (Figure 6). To the best of our knowledge, only TdaE, an acyl-CoA dehydrogenase-like flavoenzyme, has been categorized as a flavoprotein dioxygenase.[55] TdaE utilizes flavin-N5-peroxide and flavin-N5-oxide for its dioxygenase activity, a mechanism that is distinct from that of DynE13. However, the catalytic mechanisms of TdaE and DynE13 share some unmistakable similarities. The installation of the first oxygen atom for both enzymes proceeds through a flavin-(hydro)peroxo intermediate, though the (hydro)peroxo is attached to the N5 position of the flavin in TdaE and is attached to the C4 position in DynE13. The installation of the second oxygen atom in both TdaE and DynE13 involves a 1,4-Michael nucleophilic addition to their substrates by a nucleophile derived from the cosubstrate O_2 (H_2O for DynE13 and flavin-5N-O^- for TdaE). Although an alternative mechanism whereby DynE13 acts as a classic monooxygenase is also conceivable, this mechanism would entail the involvement of a second O_2 molecule and the regeneration of $FADH_2$ to generate another C4a-peroxyflavin intermediate during the enzymatic reaction. We prefer the mechanism depicted in Figure 6 due to its simplicity and alignment with existing experimental evidence that includes the ^{18}O-labeling results and the location of the catalytic residues in DynE13 and A1.

With the current information, we propose that DynA1 functions as a cofactor-independent oxygenase responsible for the installation of the third hydroxyl group at the C10 position. The intrinsic instability of the DynE13 (Int-3) product limited our ability to demonstrate the enzymatic activity of DynA1 separately, and we could confirm the enzymatic activity of DynA1 only through the DynE13-A1 coupled assay. Our proposition of DynA1 as a cofactor-free oxygenase is primarily grounded in the following considerations: First, DynA1 shares significant sequence homology and structural similarity with several AclR/SnoaL-like cofactor-independent oxygenases, including AclR, SnoL, and IdmH.[31,32] Second, oxygenases usually use flavin or pterin cofactors to stabilize resonance-stabilized semiquinone radicals, which are crucial for O_2 reduction through single electron transfers. However, when an enzymatic substrate possesses a π-conjugation system, the cofactor becomes dispensable as the substrate can form a stable radical to reduce O_2.[56−59] The putative product of DynE13 exhibits such an ideal π-conjugation system for radical formation, leading us to speculate earlier that certain AQE biosynthetic enzymes might function as cofactor-free oxygenases.[22] Indeed, the recent work by Shen and colleagues unveiled two cofactor-independent oxygenases responsible for modifying the F-ring of the AQE tiancimycins.[17] We propose that DynA1 oxygenates its substrate using a mechanism similar to ActVA-Orf6 monooxygenase (Figure 6).[49] We surmise that the dihydroxy substrate first reduces O_2 via a proton-coupled electron transfer (PCET) process with the assistance of a water molecule. The PCET process generates a triplet diradical on the OOH and substrate. This triplet diradical undergoes degeneration to form the singlet diradical (Int-4) which combines to form a hydroperoxyl intermediate (Int-5). Dissociation of the hydroperoxyl intermediate yields the final product hydroxyanthraquinone. Given the essentiality and location of T77 in the active site of DynA1 (Figure 5e), T77 may play an important role in maintaining the hydrogen bonding network required for O_2 positioning and activation, similar to the role of Asn62 in ActVA-Orf6 monooxygenase.[49] Lastly, the observation that DynA1 converted anthrone to the dimeric bianthronyl under aerobic conditions suggests that DynA1 is likely to promote the oxidative formation of a carbon-centered radical at position C10 (Figure S9), which is in line with the proposed mechanism for DynA1 (Figure 6).

In conclusion, we have successfully reconstituted the enzymatic activity of two key AQE biosynthetic enzymes: flavin-dependent oxygenase DynE13 and cofactor-free oxygenase DynA1. The two enzymes act in tandem to convert the δ-thiolactone anthracene moiety into the characteristic hydroxyanthraquinone. The multistep chemical transformation catalyzed by the DynE13−DynA1 pair involves the installation of two hydroxy groups by DynE13 with simultaneous desulfurization and decarboxylation and the installation of the third hydroxy group by the cofactor-free oxygenase DynA1. These findings enrich our understanding of enzymatic oxygenation strategies and bring us a step closer to unraveling the intriguing biosynthetic mechanism of AQEs.

■ ASSOCIATED CONTENT

Supporting Information

The Supporting Information is available free of charge at https://pubs.acs.org/doi/10.1021/jacsau.4c00279.

Strains and media; plasmid construction; preparation of cell-free extracts; cell-free protein synthesis of DynE13 and DynA1; *in vivo* protein expression and purification of recombinant DynE13 and DynA1; analytical size-exclusion chromatography; crystallization, data collection, structural determination, and refinement of DynA1; crystal structure of DynA1; enzymatic activity assays of DynE13 and DynA1; analytical methods; $^{18}O_2$- and $H_2{}^{18}O$-labeling experiments; detection of the byproduct H_2S using the MBB method; feeding experiments with substrate **5**; molecular modeling and docking; list of strains and plasmids used in this study; primer pairs used for protein overexpression and mutagenesis; codon-optimized DNA sequences of *dynE13* and *dynA1*; X-ray crystallography data collection and structure refinement statistics; dynemicins reported from *M. chersina*; biosynthetic origin of dynemicins; sungeidines produced by the Sgd pathway in *Micromonospora* sp. MD118A; proposed biosynthetic pathway for AQEs; structural characterization of product **6**; MS/MS analysis of product **6**; proposed structure for product **9**; feeding experiments with **5**; derivatization MBB method for quantifiable detection of H_2S; enzyme-based *in situ* detection of the H_2S byproduct; DynA1-catalyzed conversion of anthrone **11** to the dimeric product **11a**; selected flavin-dependent decarboxylating hydroxylases that are homologous to DynE13 and their catalytic reactions; SDS-PAGE gel and size-exclusion chromatography analyses of recombinant DynA1 and the SUMO-

https://doi.org/10.1021/jacsau.4c00279
JACS Au 2024, 4, 2925−2935

and $(His)_6$-tagged DynE13; cofactor analysis of recombinant DynE13; sequence alignments of DynE13 and DynA1 with their homologues encoded by known AQE BGCs; structural model of DynE13; crystal structure of DynA1 (PDF)

AUTHOR INFORMATION

Corresponding Authors

Jian Li − *School of Physical Science and Technology, ShanghaiTech University, Shanghai 201210, China;* orcid.org/0000-0003-2359-238X; Email: lijian@shanghaitech.edu.cn

Zhao-Xun Liang − *School of Biological Sciences, Nanyang Technological University, Singapore 637551, Singapore;* orcid.org/0000-0002-3128-1330; Email: zxliang@ntu.edu.sg

Authors

Guang-Lei Ma − *School of Biological Sciences, Nanyang Technological University, Singapore 637551, Singapore; College of Pharmaceutical Sciences, Zhejiang University, Hangzhou 310058, China; National Key Laboratory of Chinese Medicine Modernization, Innovation Center of Yangtze River Delta, Zhejiang University, Jiaxing 314100, China*

Wan-Qiu Liu − *School of Physical Science and Technology, ShanghaiTech University, Shanghai 201210, China*

Huawei Huang − *School of Biological Sciences, Nanyang Technological University, Singapore 637551, Singapore*

Xin-Fu Yan − *School of Biological Sciences, Nanyang Technological University, Singapore 637551, Singapore*

Wei Shen − *National Key Laboratory of Chinese Medicine Modernization, Innovation Center of Yangtze River Delta, Zhejiang University, Jiaxing 314100, China*

Surawit Visitsatthawong − *School of Biomolecular Science and Engineering, Vidyasirimedhi Institute of Science and Technology (VISTEC), Wangchan Valley, Rayong 21210, Thailand*

Kridsadakorn Prakinee − *School of Biomolecular Science and Engineering, Vidyasirimedhi Institute of Science and Technology (VISTEC), Wangchan Valley, Rayong 21210, Thailand;* orcid.org/0000-0003-2421-1518

Hoa Tran − *School of Biological Sciences, Nanyang Technological University, Singapore 637551, Singapore*

Xiaohui Fan − *College of Pharmaceutical Sciences, Zhejiang University, Hangzhou 310058, China; National Key Laboratory of Chinese Medicine Modernization, Innovation Center of Yangtze River Delta, Zhejiang University, Jiaxing 314100, China;* orcid.org/0000-0002-6336-3007

Yong-Gui Gao − *School of Biological Sciences, Nanyang Technological University, Singapore 637551, Singapore*

Pimchai Chaiyen − *School of Biomolecular Science and Engineering, Vidyasirimedhi Institute of Science and Technology (VISTEC), Wangchan Valley, Rayong 21210, Thailand;* orcid.org/0000-0002-8533-1604

Complete contact information is available at: https://pubs.acs.org/10.1021/jacsau.4c00279

Author Contributions

#G.-L.M. and W.-Q.L. contributed equally. CRediT: **Huawei Huang** data curation, formal analysis, investigation, methodology, writing-original draft, writing-review & editing; **Xin-Fu Yan** data curation, formal analysis, investigation, methodology, validation; **Wei Shen** investigation, methodology; **Surawit Visitsatthawong** formal analysis, writing-review & editing; **Kridsadakorn Prakinee** formal analysis, writing-review & editing; **Hoa Tran** investigation, methodology; **Xiaohui Fan**, investigation, validation; **Yong-Gui Gao**data curation, formal anlysis, methodology; **Pimchi Chaiyen**, formal analysis, writing-review & editing; **Jian Li** data curation, formal analysis, investigation, methodology, writing-original draft, writing-review & editing; **Zhao-Xun Liang** formal anlysis, investigation, writing-original draft, writing-review & editing.

Notes

The authors declare no competing financial interest.

ACKNOWLEDGMENTS

We are grateful for the generous financial support from MOE (Singapore) (grant numbers RG37/23 and MOE-T2EP30221-0010, Z.-X.L.). This work is also supported by the National Natural Science Foundation of China (no. 32171427 to W.-Q.L.), the Natural Science Foundation of Zhejiang Province (no. LZ24H300001 to G.-L.M.), and the Thailand Science Research Innovation NSRF (no. B05F640089 to P.C.).

REFERENCES

(1) Yan, X. Anthraquinone-fused enediynes: discovery, biosynthesis and development. *Nat. Prod. Rep.* **2022**, *39* (3), 703−728.

(2) Konishi, M.; Ohkuma, H.; Matsumoto, K.; Tsuno, T.; Kamei, H.; Miyaki, T.; Oki, T.; Kawaguchi, H.; VanDuyne, G. D.; Clardy, J. Dynemicin A, a novel antibiotic with the anthraquinone and 1,5-diyn-3-ene subunit. *J. Antibiot.* **1989**, *42* (9), 1449−1452.

(3) Liang, Z. X. Complexity and simplicity in the biosynthesis of enediyne natural products. *Nat. Prod. Rep.* **2010**, *27* (4), 499−528.

(4) Ando, T.; Ishii, M.; Kajiura, T.; Kameyama, T.; Miwa, K.; Sugiura, Y. A new non-protein enediyne antibiotic N1999A2: Unique enediyne chromophore similar to neocarzinostatin and DNA cleavage feature. *Tetrahedron Lett.* **1998**, *39* (36), 6495−6498.

(5) Smith, A. L.; Nicolaou, K. C. The enediyne antibiotics. *J. Med. Chem.* **1996**, *39* (11), 2103−2117.

(6) Nicolaou, K. C.; Smith, A. L.; Yue, E. W. Chemistry and biology of natural and designed enediynes. *Proc. Natl. Acad. Sci. U S A* **1993**, *90* (13), 5881−5888.

(7) Lee, M. D.; Dunne, T. S.; Chang, C. C.; Siegel, M. M.; Morton, G. O.; Ellestad, G. A.; McGahren, W. J.; Borders, D. B. Calicheamicins, a novel family of antitumor antibiotics. 4. Structure elucidation of calicheamicins. beta.1Br, gamma.1Br, alpha.2I, alpha.3I, beta.1I, gamma.1I, and delta.1I. *J. Am. Chem. Soc.* **1992**, *114* (3), 985−997.

(8) Igarashi, M.; Sawa, R.; Umekita, M.; Hatano, M.; Arisaka, R.; Hayashi, C.; Ishizaki, Y.; Suzuki, M.; Kato, C. Sealutomicins, new enediyne antibiotics from the deep-sea *actinomycete Nonomuraea* sp. MM565M-173N2. *J. Antibiot.* **2021**, *74* (5), 291−299.

(9) Davies, J.; Wang, H.; Taylor, T.; Warabi, K.; Huang, X. H.; Andersen, R. J. Uncialamycin, a new enediyne antibiotic. *Org. Lett.* **2005**, *7* (23), 5233−5236.

(10) Konishi, M.; Ohkuma, H.; Tsuno, T.; Oki, T.; VanDuyne, G. D.; Clardy, J. Crystal and molecular structure of dynemicin A: a novel 1,5-diyn-3-ene antitumor antibiotic. *J. Am. Chem. Soc.* **1990**, *112* (9), 3715−3716.

(11) Yan, X.; Chen, J. J.; Adhikari, A.; Yang, D.; Crnovcic, I.; Wang, N.; Chang, C. Y.; Rader, C.; Shen, B. Genome mining of *Micromonospora yangpuensis* DSM 45577 as a producer of an anthraquinone-fused enediyne. *Org. Lett.* **2017**, *19* (22), 6192−6195.

(12) Yan, X.; Ge, H.; Huang, T.; Hindra; Yang, D.; Teng, Q.; Crnovčić, I.; Li, X.; Rudolf, J. D.; Lohman, J. R.; Gansemans, Y.; Zhu, X.; Huang, Y.; Zhao, L. X.; Jiang, Y.; Van Nieuwerburgh, F.; Rader,

C.; Duan, Y.; Shen, B. Strain prioritization and genome mining for enediyne natural products. *MBio* **2016**, *7* (6), No. e02104.
(13) Tuttle, T.; Kraka, E.; Thiel, W.; Cremer, D. A QM/MM study of the Bergman reaction of dynemicin A in the minor groove of DNA. *J. Phys. Chem. B* **2007**, *111* (28), 8321−8328.
(14) Sugiura, Y.; Shiraki, T.; Konishi, M.; Oki, T. DNA intercalation and cleavage of an antitumor antibiotic dynemicin that contains anthracycline and enediyne cores. *Proc. Natl. Acad. Sci. U S A* **1990**, *87* (10), 3831−3835.
(15) Sugiura, Y.; Arakawa, T.; Uesugi, M.; Shiraki, T.; Ohkuma, H.; Konishi, M. Reductive and nucleophilic activation products of dynemicin A with methyl thioglycolate. A rational mechanism for DNA cleavage of the thiol-activated dynemicin A. *Biochemistry* **1991**, *30* (12), 2989−2992.
(16) Snyder, J. P.; Tipsword, G. E. Proposal for blending classical and biradical mechanisms in antitumor antibiotics: dynemicin A. *J. Am. Chem. Soc.* **1990**, *112* (10), 4040−4042.
(17) Gui, C.; Kalkreuter, E.; Liu, Y. C.; Li, G.; Steele, A. D.; Yang, D.; Chang, C.; Shen, B. Cofactorless oxygenases guide anthraquinone-fused enediyne biosynthesis. *Nat. Chem. Biol.* **2024**, *20* (2), 243−250.
(18) Pal, P.; Wessely, S. M. L.; Townsend, C. A. Normal and aberrant methyltransferase activities give insights into the final steps of dynemicin A biosynthesis. *J. Am. Chem. Soc.* **2023**, *145* (23), 12935−12947.
(19) Pal, P.; Alley, J. R.; Townsend, C. A. Examining heterodimerization by aryl C-N coupling in dynemicin biosynthesis. *ACS Chem. Biol.* **2023**, *18* (2), 304−314.
(20) Gui, C.; Kalkreuter, E.; Liu, Y. C.; Adhikari, A.; Teijaro, C. N.; Yang, D.; Chang, C.; Shen, B. Intramolecular C-C bond formation links anthraquinone and enediyne scaffolds in tiancimycin biosynthesis. *J. Am. Chem. Soc.* **2022**, *144* (44), 20452−20462.
(21) Bhardwaj, M.; Cui, Z.; Daniel Hankore, E.; Moonschi, F. H.; Saghaeiannejad Esfahani, H.; Kalkreuter, E.; Gui, C.; Yang, D.; Phillips, G. N. Jr.; Thorson, J. S.; Shen, B.; Van Lanen, S. G. A discrete intermediate for the biosynthesis of both the enediyne core and the anthraquinone moiety of enediyne natural products. *Proc. Natl. Acad. Sci. U S A* **2023**, *120* (9), No. e2220468120.
(22) Ma, G. L.; Tran, H. T.; Low, Z. J.; Candra, H.; Pang, L. M.; Cheang, Q. W.; Fang, M.; Liang, Z. X. Pathway retrofitting yields insights into the biosynthesis of anthraquinone-fused enediynes. *J. Am. Chem. Soc.* **2021**, *143* (30), 11500−11509.
(23) Cohen, D. R.; Townsend, C. A. C-N-coupled metabolites yield insights into dynemicin A biosynthesis. *Chembiochem* **2020**, *21* (15), 2137−2142.
(24) Cohen, D. R.; Townsend, C. A. A dual role for a polyketide synthase in dynemicin enediyne and anthraquinone biosynthesis. *Nat. Chem.* **2018**, *10* (2), 231−236.
(25) Cohen, D. R.; Townsend, C. A. Characterization of an anthracene intermediate in dynemicin biosynthesis. *Angew. Chem., Int. Ed. Engl.* **2018**, *57* (20), 5650−5654.
(26) Gao, Q.; Thorson, J. S. The biosynthetic genes encoding for the production of the dynemicin enediyne core in Micromonospora chersina ATCC53710. *FEMS Microbiol. Lett.* **2008**, *282* (1), 105−114.
(27) Liew, C. W.; Nilsson, M.; Chen, M. W.; Sun, H.; Cornvik, T.; Liang, Z.-X.; Lescar, J. Crystal structure of the acyltransferase domain of the iterative polyketide synthase in enediyne biosynthesis. *J. Biol. Chem.* **2012**, *287* (27), 23203−23215.
(28) Sun, H.; Kong, R.; Zhu, D.; Lu, M.; Ji, Q.; Liew, C. W.; Lescar, J.; Zhong, G.; Liang, Z. X. Products of the iterative polyketide synthases in 9- and 10-membered enediyne biosynthesis. *Chem. Commun.* **2009**, *47*, 7399−7401.
(29) Bringmann, G.; Noll, T. F.; Gulder, T. A.; Grune, M.; Dreyer, M.; Wilde, C.; Pankewitz, F.; Hilker, M.; Payne, G. D.; Jones, A. L.; Goodfellow, M.; Fiedler, H. P. Different polyketide folding modes converge to an identical molecular architecture. *Nat. Chem. Biol.* **2006**, *2* (8), 429−433.
(30) Low, Z. J.; Ma, G. L.; Tran, H. T.; Zou, Y.; Xiong, J.; Pang, L.; Nuryyeva, S.; Ye, H.; Hu, J. F.; Houk, K. N.; Liang, Z. X. Sungeidines from a non-canonical enediyne biosynthetic pathway. *J. Am. Chem. Soc.* **2020**, *142* (4), 1673−1679.
(31) Beinker, P.; Lohkamp, B.; Peltonen, T.; Niemi, J.; Mantsala, P.; Schneider, G. Crystal structures of SnoaL2 and AclR: two putative hydroxylases in the biosynthesis of aromatic polyketide antibiotics. *J. Mol. Biol.* **2006**, *359* (3), 728−740.
(32) Sultana, A.; Kallio, P.; Jansson, A.; Wang, J. S.; Niemi, J.; Mäntsälä, P.; Schneider, G. Structure of the polyketide cyclase SnoaL reveals a novel mechanism for enzymatic aldol condensation. *EMBO J.* **2004**, *23* (9), 1911−1921.
(33) Ji, X.; Liu, W.-Q.; Li, J. Recent advances in applying cell-free systems for high-value and complex natural product biosynthesis. *Curr. Opin. Microbiol.* **2022**, *67*, No. 102142.
(34) Silverman, A. D.; Karim, A. S.; Jewett, M. C. Cell-free gene expression: an expanded repertoire of applications. *Nat. Rev. Genet.* **2020**, *21* (3), 151−170.
(35) Liu, W.-Q.; Zhang, L.; Chen, M.; Li, J. Cell-free protein synthesis: Recent advances in bacterial extract sources and expanded applications. *Biochem. Eng. J.* **2019**, *141*, 182−189.
(36) Otto, K.; Hofstetter, K.; Röthlisberger, M.; Witholt, B.; Schmid, A. Biochemical characterization of StyAB from Pseudomonas sp. strain VLB120 as a two-component flavin-diffusible monooxygenase. *J. Bacteriol.* **2004**, *186* (16), 5292−5302.
(37) De Marco, A.; Deuerling, E.; Mogk, A.; Tomoyasu, T.; Bukau, B. Chaperone-based procedure to increase yields of soluble recombinant proteins produced in *E. coli*. *BMC Biotechnol.* **2007**, *7* (1), 32.
(38) Paul, C. E.; Tischler, D.; Riedel, A.; Heine, T.; Itoh, N.; Hollmann, F. Nonenzymatic regeneration of styrene monooxygenase for catalysis. *ACS Catal.* **2015**, *5* (5), 2961−2965.
(39) Mondal, P.; Roy, S.; Loganathan, G.; Mandal, B.; Dharumadurai, D.; Akbarsha, M. A.; Sengupta, P. S.; Chattopadhyay, S.; Guin, P. S. 1-Amino-4-hydroxy-9,10-anthraquinone − An analogue of anthracycline anticancer drugs, interacts with DNA and induces apoptosis in human MDA-MB-231 breast adinocarcinoma cells: Evaluation of structure−activity relationship using computational, spectroscopic and biochemical studies. *Biochem. Biophys. Rep.* **2015**, *4*, 312−323.
(40) Caldara-Festin, G.; Jackson, D. R.; Barajas, J. F.; Valentic, T. R.; Patel, A. B.; Aguilar, S.; Nguyen, M.; Vo, M.; Khanna, A.; Sasaki, E.; Liu, H. W.; Tsai, S. C. Structural and functional analysis of two didomain aromatase/cyclases from type II polyketide synthases. *Proc. Natl. Acad. Sci. U S A* **2015**, *112* (50), E6844−E6851.
(41) Das, A.; Khosla, C. Biosynthesis of aromatic polyketides in bacteria. *Acc. Chem. Res.* **2009**, *42* (5), 631−639.
(42) Zhang, W.; Li, Y.; Tang, Y. Engineered biosynthesis of bacterial aromatic polyketides in *Escherichia coli*. *Proc. Natl. Acad. Sci. U S A* **2008**, *105* (52), 20683−8.
(43) Fan, J.; Ran, H.; Wei, P. L.; Li, Y.; Liu, H.; Li, S. M.; Hu, Y.; Yin, W. B. Pretrichodermamide A biosynthesis reveals the hidden diversity of epidithiodiketopiperazines. *Angew. Chem., Int. Ed. Engl.* **2023**, *62* (18), No. e202217212.
(44) Qu, X.; Pang, B.; Zhang, Z.; Chen, M.; Wu, Z.; Zhao, Q.; Zhang, Q.; Wang, Y.; Liu, Y.; Liu, W. Caerulomycins and collismycins share a common paradigm for 2,2'-bipyridine biosynthesis via an unusual hybrid polyketide-peptide assembly Logic. *J. Am. Chem. Soc.* **2012**, *134* (22), 9038−9041.
(45) Shen, X.; Kolluru, G. K.; Yuan, S.; Kevil, C. G. Measurement of H2S in vivo and in vitro by the monobromobimane method. *Methods Enzymol.* **2015**, *554*, 31−45.
(46) Lynch, M. J.; Crane, B. R. Design, Validation, and Application of an enzyme-coupled hydrogen sulfide detection assay. *Biochemistry* **2019**, *58* (6), 474−483.
(47) Jumper, J.; Evans, R.; Pritzel, A.; Green, T.; Figurnov, M.; Ronneberger, O.; Tunyasuvunakool, K.; Bates, R.; Žídek, A.; Potapenko, A.; Bridgland, A.; Meyer, C.; Kohl, S. A. A.; Ballard, A. J.; Cowie, A.; Romera-Paredes, B.; Nikolov, S.; Jain, R.; Adler, J.; Back, T.; Petersen, S.; Reiman, D.; Clancy, E.; Zielinski, M.; Steinegger, M.; Pacholska, M.; Berghammer, T.; Bodenstein, S.;

https://doi.org/10.1021/jacsau.4c00279
JACS Au 2024, 4, 2925−2935

Silver, D.; Vinyals, O.; Senior, A. W.; Kavukcuoglu, K.; Kohli, P.; Hassabis, D. Highly accurate protein structure prediction with AlphaFold. *Nature* **2021**, *596* (7873), 583−589.
(48) Drulyte, I.; Obajdin, J.; Trinh, C. H.; Kalverda, A. P.; Van der Kamp, M. W.; Hemsworth, G. R.; Berry, A. Crystal structure of the putative cyclase IdmH from the indanomycin nonribosomal peptide synthase/polyketide synthase. *IUCrJ* **2019**, *6* (Pt 6), 1120−1133.
(49) Li, X.; Li, X.; Zhang, Q.; Lv, P.; Jia, Y.; Wei, D. Cofactor-free ActVA-Orf6 monooxygenase catalysisviaproton-coupled electron transfer: a QM/MM study. *Org. Biomol. Chem.* **2022**, *20* (28), 5525−5534.
(50) Siitonen, V.; Blauenburg, B.; Kallio, P.; Mantsala, P.; Metsa-Ketela, M. Discovery of a two-component monooxygenase SnoaW/SnoaL2 involved in nogalamycin biosynthesis. *Chem. Biol.* **2012**, *19* (5), 638−646.
(51) Kataoka, M.; Shimizu, S.; Yamada, H. Distribution and immunological characterization of microbial aldehyde reductases. *Arch. Microbiol.* **1992**, *157* (3), 279−283.
(52) Feilcke, R.; Arnouk, G.; Raphane, B.; Richard, K.; Tietjen, I.; Andrae-Marobela, K.; Erdmann, F.; Schipper, S.; Becker, K.; Arnold, N.; Frolov, A.; Reiling, N.; Imming, P.; Fobofou, S. A. T. Biological activity and stability analyses of knipholone anthrone, a phenyl anthraquinone derivative isolated from Kniphofia foliosa Hochst. *J. Pharm. Biomed. Anal.* **2019**, *174*, 277−285.
(53) Estanqueiro, M.; Conceição, J.; Amaral, M. H.; Lobo, J. M. S. Use of solid dispersions to increase stability of dithranol in topical formulations. *Braz. J. Pharm. Sci.* **2014**, *50*, 583−590.
(54) Grimminger, W.; Leng-Peschlow, E. Instability of rhein-9-anthrone as a problem in pharmacological and analytical use. *Pharmacol.* **1988**, *36*, 129−137.
(55) Duan, Y.; Toplak, M.; Hou, A.; Brock, N. L.; Dickschat, J. S.; Teufel, R. A flavoprotein dioxygenase steers bacterial tropone biosynthesis via coenzyme A-ester oxygenolysis and ring epoxidation. *J. Am. Chem. Soc.* **2021**, *143* (27), 10413−10421.
(56) Bugg, T. D. H. Dioxygenase enzymes: catalytic mechanisms and chemical models. *Tetrahedron* **2003**, *59* (36), 7075−7101.
(57) Fetzner, S. Oxygenases without requirement for cofactors or metal ions. *Appl. Microbiol. Biotechnol.* **2002**, *60*, 243−257.
(58) Fetzner, S.; Steiner, R. A. Cofactor-independent oxidases and oxygenases. *Appl. Microbiol. Biotechnol.* **2010**, *86* (3), 791−804.
(59) Hernández-Ortega, A.; Quesne, M. G.; Bui, S.; Heyes, D. J.; Steiner, R. A.; Scrutton, N. S.; de Visser, S. P. Catalytic mechanism of cofactor-free dioxygenases and how they circumvent spin-forbidden oxygenation of their substrates. *J. Am. Chem. Soc.* **2015**, *137* (23), 7474−7487.

https://doi.org/10.1021/jacsau.4c00279
JACS Au 2024, 4, 2925−2935